32nd International Conference
ENGINEERING MECHANICS 2026
Medlov, Czech Republic, May 11 – 13, 2026

CORRELATION OF LOCAL MICROMECHANICAL PROPERTIES WITH EDS CHEMICAL PROFILES IN BLENDED CEMENT PASTE

Špaková A.[1], **Němeček J.**[2], **Němeček J.**[3]

Abstract: *This study investigates the correlation between micromechanical properties and chemical composition in a blended cement paste containing fly ash and limestone. Micromechanical characterization was performed using grid nanoindentation with a spatial resolution of* $2.5\,\mu\mathrm{m}$ *to acquire the local Young's modulus across the different cement paste phases. Additionally, Energy Dispersive X-ray Spectroscopy (EDS) line scans provided pointwise elemental composition, enabling the calculation of (Ca–S)/Si and Al/Si ratios for each measurement location. By combining the mechanical and chemical datasets, the spatial distribution of element content and corresponding stiffness was visualized, allowing segmentation of the paste into distinct phases such as low- and high-density C–S–H, Portlandite, and fly ash regions.*

Keywords: Nanoindentation, Scanning electron microscopy, Cement Paste, Energy Dispersive X-ray Spectroscopy

1. Introduction

Cementitious materials exhibit a complex and heterogeneous microstructure composed of hydration products such as low-density Calcium Silicate Hydrate (LD C–S–H), high-density Calcium Silicate Hydrate (HD C–S–H), Portlandite (CH), and unhydrated clinker Jennings et al. (2007). When supplementary cementitious materials such as slag, fly ash, or silica fume are added, the microstructure changes significantly, and new hydration products are formed Li et al. (2021).

Nanoindentation is commonly used to characterize the micromechanical behavior of these phases Němeček et al. (2013); Luo et al. (2018); Němeček et al. (2020). In previous studies, separation into individual phases has been achieved either by statistical analysis Němeček et al. (2013) or by correlating nanoindentation data with BSE images Hilloulin et al. (2018). However, purely statistical approaches require large datasets, while BSE-based segmentation may not reliably capture the underlying phase composition, as BSE contrast alone is sometimes insufficient for accurate phase identification.

By combining nanoindentation with SEM–BSE imaging and Energy Dispersive X-ray Spectroscopy (EDS) line scans, it is possible to correlate local mechanical properties with elemental composition, enabling more reliable identification of individual cement paste phases. In particular, (Ca–S)/Si and Al/Si ratios obtained from EDS serve as effective indicators for phase differentiation, linking oxide distribution to variations in local stiffness.

Although such chemical–mechanical correlations have been applied to synthetic C–S–H and some blended pastes Pelisser et al. (2012), systematic studies integrating nanoindentation grids with SEM–EDS line scans in cement pastes containing fly ash and limestone are still limited.

In this study, a blended cement paste with fly ash and limestone is investigated. By mapping local Young's modulus alongside chemical composition, individual phases can be identified, and the influence of oxide distributions on micromechanical behavior is revealed.

[1] Bc. Andrea Špaková, Orcid 0009-0008-2784-3995: Department of Mechanics, Faculty of Civil Engineering, Czech Technical University, Thákurova 2077/7; 166 29, Prague 6; CZ, spakoand@student.cvut.cz

[2] Ing. Jiří Němeček, Ph.D., Orcid 0000-0002-5635-695X: Department of Mechanics, Faculty of Civil Engineering, Czech Technical University, Thákurova 2077/7; 166 29, Prague 6; CZ, jiri.nemecek.1@fsv.cvut.cz

[3] Prof. Ing. Jiří Němeček, Ph.D., DSc., Orcid 0000-0002-3565-8182: Department of Mechanics, Faculty of Civil Engineering, Czech Technical University, Thákurova 2077/7; 166 29, Prague 6; CZ, jiri.nemecek@fsv.cvut.cz

ISSN: 1805-8256, doi: 10.21495/em2026-133

2. Experiments and methods

2.1. Sample preparation

A cement paste with a water–cement ratio of 0.5 was prepared using blended Portland cement CEM II/B-M (V-LL) 32.5 R with an addition of 18 wt.% fly ash. The prepared paste mixture was poured into plastic cylindrical molds of 27 mm diameter and 70 mm height, followed by mechanical vibration. Once hardened, the samples were removed from the molds and cut to a height of approximately 19 mm using a Struers Secotom-50 diamond saw.

The sample surfaces were polished for nanoindentation and SEM analysis using a multi-step polishing procedure with SiC foils of grit sizes from 1200 to 4000 on a Struers Tegramin 20 machine, following the procedure described in Němeček et al. (2020).

2.2. Nanoindentation

Nanoindentation was conducted using a Hysitron TI-980 equipped with a Berkovich diamond tip. Eight grids of 22 × 22 indents, with a spacing of 2.5 µm, were performed on the sample using accelerated property mapping with a trapezoidal loading protocol, each test lasting 0.1 s as described in Němeček et al. (2020). Young's modulus, E, was evaluated from the measured load-displacement curves using the method of Oliver and Pharr (1992). An example of a performed mechanical map is shown in Fig. 1.

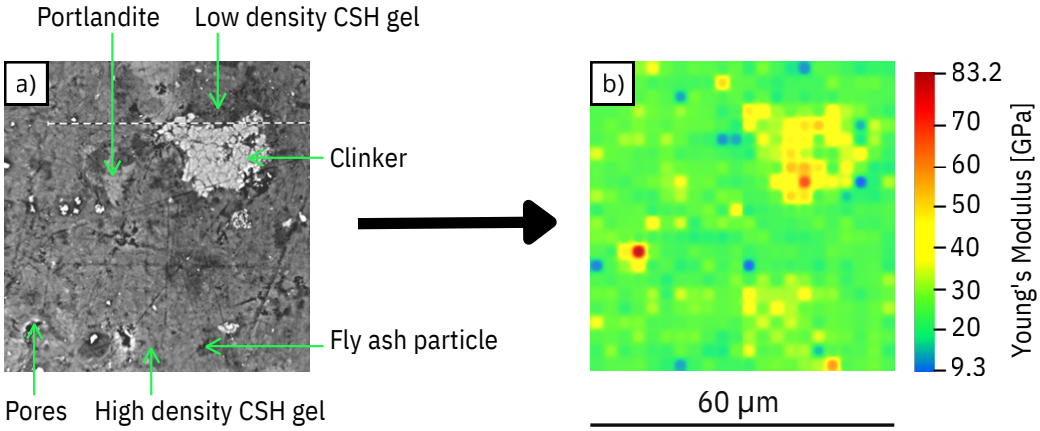

Fig. 1: a) SEM–BSE image of the cement paste area subjected to nanoindentation, with individual cement phases identified; b) Visual Young's modulus map of the same area.

2.3. Energy Dispersive X-ray Spectroscopy

SEM–BSE images at 2000× magnification, with a size of 110×110 µm^2, were taken to perform EDS line scans along the 60 µm lines of mechanical indents location. The scans were acquired with a pixel resolution of 107 nm, using 10 passes at a scanning velocity of 10 ms per pixel, with a BSD full detector and an accelerating voltage of 15 kV. Fig. 2 shows the overlap of the SEM–BSE and mechanical maps.

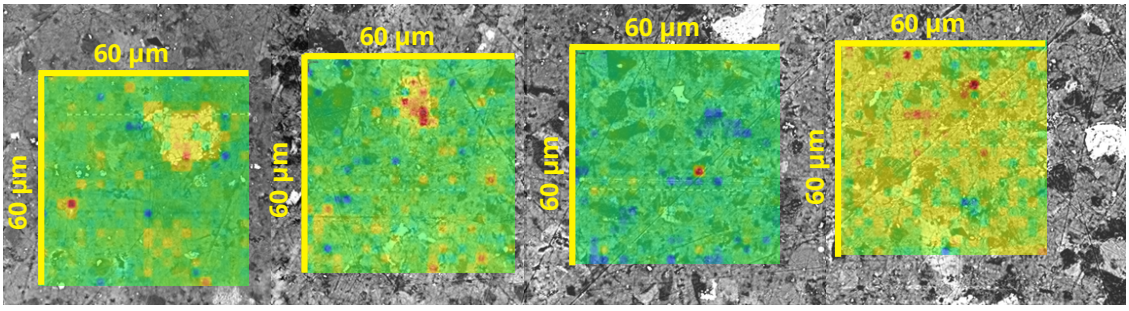

Fig. 2: Overlap of SEM-BSE images and the area of nanoindented grids of the tested sample.

3. Results and discussion

Fig. 3 presents the line profiles results of the elemental composition of Ca, Si, S, and Al obtained from EDS line scans, the calculated (Ca–S)/Si and Al/Si ratios, the BSE image, and the local Young's modulus values from nanoindentation. Based on all these line profiles, the segmentation into individual phases was performed. This procedure enabled the identification of distinct cement paste phases, including HD C-S-H, LD C-S-H gels, CH, and hydrated fly ash with Al content above and below 9%.

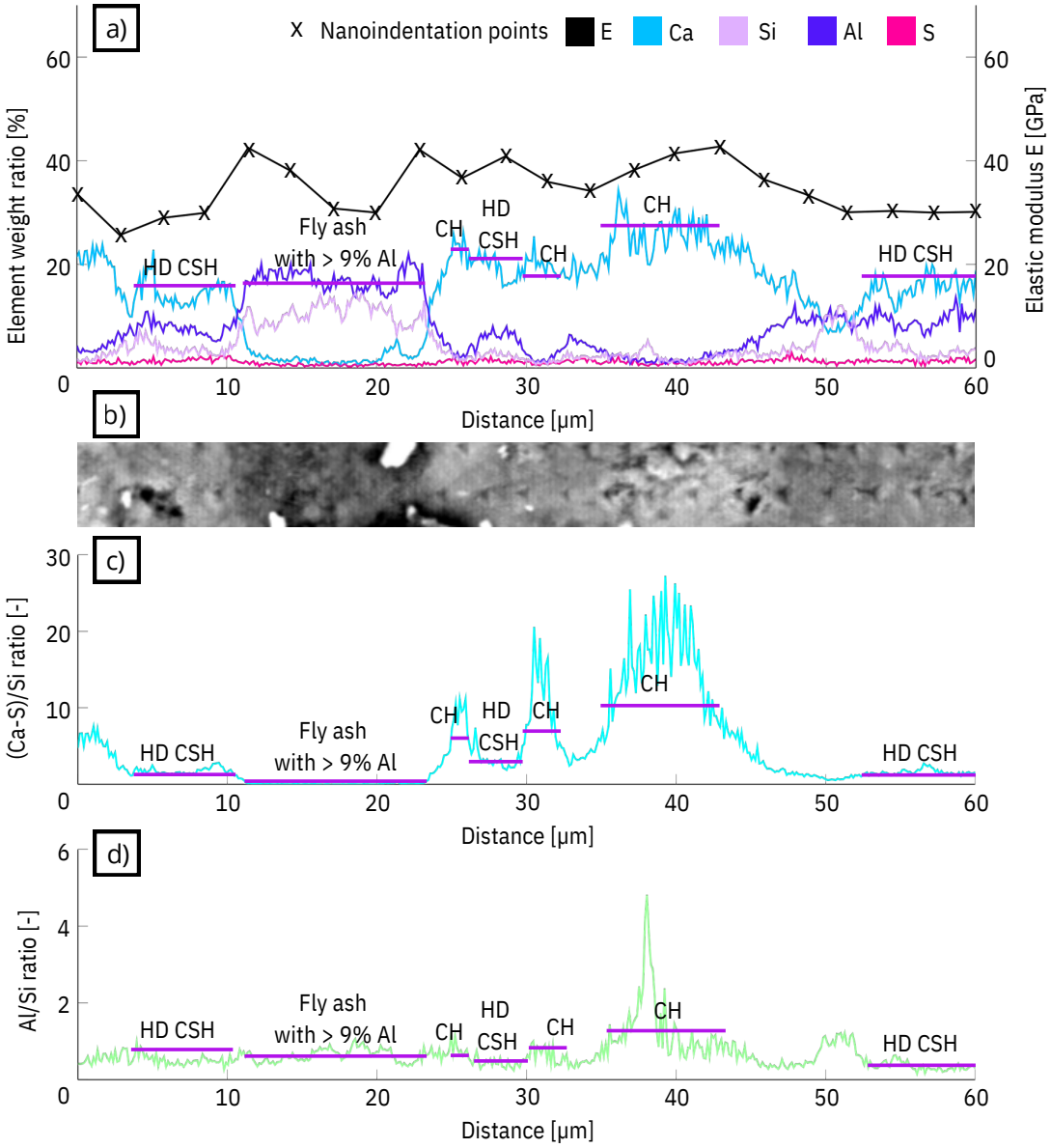

Fig. 3: a) Element profiles from EDS line scans with corresponding Young's modulus values measured at the nanoindentation points along the same profile; b) SEM–BSE image showing the EDS line scan; c) (Ca–S)/Si and d) Al/Si ratios calculated from the EDS data along the nanoindentation profile.

The mean values of the separated phases are summarized in Table 1. The differences in micromechanical behavior of the individual phases correlate well with variations in chemical composition. In particular, fly ash with high Al content (>9%) exhibits a lower Young's modulus (24.4 GPa) compared to fly ash with low Al content (<9%) (32.4 GPa), which is also reflected in the (Ca–S)/Si and Al/Si ratios. The Young's modulus values of the separated phases are consistent with literature reports Hu (2015); Zhu et al. (2007); Mondal et al. (2007); Jennings et al. (2007).

Specifically, the Young's modulus of LD C–S–H gel measured in this study (24.9 $\pm$ 0.3 GPa) closely matches Hu's reported value of 25 GPa for a cement paste with a water-to-cement ratio of 0.4. Similarly,

the HD C–S–H gel exhibits a modulus of 31.2 ± 2.9 GPa, compared to Hu's 30.9 GPa. Furthermore, the stiffness of portlandite in this study (36.4 ± 3.4 GPa) is in close agreement with literature-reported values of 36–43 GPa Hu (2015); Mondal et al. (2007).

Tab. 1: Correlation results of nonoindentation and EDS line scans for various cement phases.

	C-S-H gel		Portlandite	Fly ash content with	
Observed property [%]	low density	high density	-	< 9% Al	> 9% Al
E [GPa]	24.9 ± 0.3	31.2 ± 2.9	36.4 ± 3.4	32.4 ±6.1	24.4± 4.0
(Ca-S)/Si ratio [-]	2.07 ± 0.41	2.82 ± 1.26	14.98 ± 3.16	0.015 ± 0.13	9.48 ± 0.35
Al/Si ratio [-]	0.84 ± 0.35	0.56 ± 0.28	0.58 ± 0.30	0.88 ± 0.38	5.83 ± 0.34

4. Conclusions

This study demonstrates that combining local chemical composition analysis (Ca, Si, S, and Al) from EDS line scans with BSE imaging is highly effective for distinguishing micromechanical properties in blended cement paste. The calculated (Ca–S)/Si and Al/Si ratios served as reliable indicators for phase identification, enabling segmentation into distinct phases such as LD and HD C–S–H gels, Portlandite, and hydrated fly ash. The measured Young's modulus values (LD C–S–H: 24.9 ± 0.3 GPa; HD C–S–H: 31.2 ± 2.9 GPa; Portlandite: 36.4 ± 3.4 GPa) are in close agreement with literature, validating the approach.

Acknowledgments

This work was financially supported by the Czech Science Foundation under grant number 26-22195S and Grant Agency of the Czech Technical University in Prague (SGS25/083/OHK1/2T/11).

References

Hilloulin, B., Robira, M., and Loukili, A. (2018) Coupling statistical indentation and microscopy to evaluate micromechanical properties of materials: Application to viscoelastic behavior of irradiated mortars. *Cement and Concrete Composites*, 94, pp. 153–165.

Hu, C. (2015) Nanoindentation as a tool to measure and map mechanical properties of hardened cement pastes. *MRS Communications*, 5, 1, pp. 83–87.

Jennings, H. M., Thomas, J. J., Gevrenov, J. S., Constantinides, G., and Ulm, F.-J. (2007) A multi-technique investigation of the nanoporosity of cement paste. *Cement and Concrete Research*, 37, 3, pp. 329–336.

Li, L., Yang, J., Li, H., and Du, Y. (2021) Insights into the microstructure evolution of slag, fly ash and condensed silica fume in blended cement paste. *Construction and Building Materials*, 309, pp. 125044.

Luo, Z., Li, W., Wang, K., and Shah, S. P. (2018) Research progress in advanced nanomechanical characterization of cement-based materials. *Cement and Concrete Composites*, 94, pp. 277–295.

Mondal, P., Shah, S. P., and Marks, L. (2007) A reliable technique to determine the local mechanical properties at the nanoscale for cementitious materials. *Cement and Concrete Research*, 37, 10, pp. 1440–1444.

Němeček, J., Králík, V., and Vondřejc, J. (2013) Micromechanical analysis of heterogeneous structural materials. *Cement and Concrete Composites*, 36, pp. 85–92.

Němeček, J., Lukeš, J., and Němeček, J. (2020) High-speed mechanical mapping of blended cement pastes and its comparison with standard modes of nanoindentation. *Materials Today Communications*, 23, pp. 100806.

Oliver, W. and Pharr, G. (1992) An improved technique for determining hardness and elastic modulus using load and displacement sensing indentation experiments. *Journal of materials research*, 7, 6, pp. 1564–1583.

Pelisser, F., Gleize, P. J. P., and Mikowski, A. (2012) Effect of the ca/si molar ratio on the micro/nanomechanical properties of synthetic csh measured by nanoindentation. *The Journal of physical chemistry C*, 116, 32, pp. 17219–17227.

Zhu, W., Hughes, J. J., Bicanic, N., and Pearce, C. J. (2007) Nanoindentation mapping of mechanical properties of cement paste and natural rocks. *Materials characterization*, 58, 11-12, pp. 1189–1198.